LNF-95/060

Photon Polarization Properties in Laser Backscattering

D. Babusci, G. Giordano, G. Matone

Physics Letters , 355, 1-8, (1995)

ELSEVIER

27 July 1995

Physics Letters B 355 (1995) 1–8

PHYSICS LETTERS B

Photon polarization properties in laser backscattering

D. Babusci, G. Giordano, G. Matone

INFN - Laboratori Nazionali di Frascati, P.O. Box 13, I-00044 Frascati (Roma), Italy

Received 10 April 1995
Editor: G.F. Bertsch

Abstract

In this paper we present the full calculation of the final photon polarization in the Compton scattering on electron $\gamma + e \to \gamma + e$. We claim to be in disagreement with some of the results quoted by F.R. Arutyunian and V.A. Tumanian in Sov. Phys. Usp. 83 (1964) 339; Phys. Lett. 4 (1963) 177.

1. Introduction

A general discussion of the polarization effects in Compton scattering can be found in Ref. [1] and in several other review articles published elsewhere [2–5]. The polarization of the final photon is particularly relevant in the experiments where high energy polarized photons are produced by the backscattering of laser light against high energy electrons in a storage ring [6,7]. As a matter of fact, since the electron spin-flip amplitude vanishes in the backward direction, the final photons retain almost entirely the initial laser polarization. However, at other angles the photon polarization can change due to the role of orbital angular momentum. The knowledge of the average value of the final photon polarization is essential for any experimental activity with the backscattered photon beam.

After a short summary of the basic theoretical formulas, we derive the expressions of all the quantities of interest in the general case where the initial electron is arbitrarily polarized. In particular we find that some of the final photon polarization parameters quoted by F.R. Arutyunian and V.A. Tumanian in Ref. [4] (in the following referred to as AT) are wrong. The correct expressions are here presented and discussed.

2. The Compton process

The kinematics of the process can be described by the usual (s, t, u)-variables. By indicating with $k(k')$ and p the 4-momenta of the initial (final) photon and electron, respectively, one has:

$$s - m^2 = \tilde{s} = 2pk$$
$$t = -2kk' \qquad (\tilde{s} + t + \tilde{u} = 0)$$
$$u - m^2 = \tilde{u} = -2pk'$$

The scattering amplitude can be conveniently discussed by introducing the Stokes parameters of the incoming photon ($\xi_k^{(i)}$) and those associated with the polarization detector (σ_k) ($k = 1, 2, 3$). In our conventions the first and third parameters determine the probabilities of two linear polarizations which make an angle of $\pi/4$ with each other and the second parameter refers to the circular polarization. The polarization degrees are defined as follows:

Elsevier Science B.V.
SSDI 0370-2693(95)00719-9

$$P_l = \sqrt{\xi_1^2 + \xi_3^2}\,, \quad P_c = |\xi_2|\,, \quad P = \sqrt{P_l^2 + P_c^2} \quad (2.1)$$

and are separately Lorentz-invariant quantities [1].

By referring the Stokes "vector" of the incoming photon to the unit vectors

$$\hat{\chi}_1^{(i)} = \frac{\boldsymbol{k} \times \boldsymbol{k}'}{|\boldsymbol{k} \times \boldsymbol{k}'|}\,, \quad \hat{\chi}_2^{(i)} = \frac{\boldsymbol{k} \times \hat{\chi}_1^{(i)}}{|\boldsymbol{k} \times \hat{\chi}_1^{(i)}|} \quad (2.2)$$

and summing over the final electron polarization states, the squared amplitude can be written as

$$|\mathcal{M}|^2 = 16\pi^2 e^4 \{ F_0 + (\boldsymbol{\xi}^{(i)} \cdot \boldsymbol{F}) + (\boldsymbol{\sigma} \cdot \boldsymbol{F}') + (\boldsymbol{\sigma} \cdot T\boldsymbol{\xi}^{(i)}) \} \quad (2.3)$$

where the coefficient F_0 and the components of the vectors $\boldsymbol{F}$ and $\boldsymbol{F}'$ are given by

$$F_0 = 4m^2 a\,(1 + m^2 a) - b$$

$$F_1 = 0\,, \quad F_1' = F_1$$

$$F_2 = -2ma\,\{ (1 + 2m^2 a)\,(kw) + (k'w) \}$$

$$F_2' = F_2\,(k \leftrightarrow k')$$

$$F_3 = -4m^2 a\,(1 + m^2 a)\,, \quad F_3' = F_3$$

and the T-matrix is defined by the following elements:

$$T_{11} = 2\,(1 + 2m^2 a)\,, \quad T_{22} = -\frac{b}{2} T_{11}\,, \quad T_{33} = 2 - F_3$$

$$T_{12} = \frac{\tilde{s}}{\tilde{u}} T_{21} = -4\,\frac{m}{\tilde{u}}\,a\,\epsilon^{\mu\nu\lambda\eta}\,p_\mu w_\nu k_\lambda k'_\eta\,, \quad T_{13} = T_{31} = 0$$

$$T_{23} = ma\,\{ 2\frac{\tilde{u}}{\tilde{s}}\,(kw) + T_{11}\,(k'w) \}$$

$$T_{32} = ma\,\{ T_{11}\,(kw) + 2\frac{\tilde{s}}{\tilde{u}}\,(k'w) \}$$

In these equations a and b are

$$a = \frac{1}{\tilde{s}} + \frac{1}{\tilde{u}}\,, \quad b = \frac{\tilde{s}}{\tilde{u}} + \frac{\tilde{u}}{\tilde{s}}$$

w is the spin 4-vector of the initial electron defined by the conditions

$$w_\mu p^\mu = 0\,, \quad w_\mu w^\mu = -\boldsymbol{\zeta}^2$$

and $\boldsymbol{\zeta}/2$ is the spin of the electron in the electron rest frame (ERF system).

Eq. (2.3) can be compacted in the following form:

$$|\mathcal{M}|^2 = \frac{1}{2}\,|\bar{\mathcal{M}}|^2 \{ 1 + (\boldsymbol{\sigma} \cdot \boldsymbol{\xi}^{(f)}) \} \quad (2.4)$$

where

$$\boldsymbol{\xi}^{(f)} = (\xi_1^{(f)}, \xi_2^{(f)}, \xi_3^{(f)}) = \frac{1}{A_0}\,(\boldsymbol{F}' + T\boldsymbol{\xi}^{(i)}) \quad (2.5)$$

is the Stokes "vector" of the final photon. This vector is referred to the unit vector base

$$\hat{\chi}_1^{(f)} = \hat{\chi}_1^{(i)}\,, \quad \hat{\chi}_2^{(f)} = \frac{\boldsymbol{k}' \times \hat{\chi}_1^{(f)}}{|\boldsymbol{k}' \times \hat{\chi}_1^{(f)}|} \quad (2.6)$$

which should not be confused with that of Eq. (2.2) defined for the initial photon. The presence of the scalar product $\boldsymbol{\sigma} \cdot \boldsymbol{\xi}^{(f)}$ allows to determine the photon flux in any given polarization channel, by selecting the appropriate value of the detector Stokes "vector" $\boldsymbol{\sigma}$ in Eq. (2.4). Moreover, the squared amplitude summed over the polarization states of the final photon can be obtained by imposing $\boldsymbol{\sigma} = 0$ and multiplying by a factor 2 the expression of Eq. (2.3)

$$|\bar{\mathcal{M}}|^2 = 32\pi^2 e^4 \{ F_0 + (\boldsymbol{\xi}^{(i)} \cdot \boldsymbol{F}) \} = 32\pi^2 e^4 A_0 \quad (2.7)$$

The cross-section associated to this squared amplitude is the usual Klein-Nishina formula [1–3] ($r_0 = e^2/m$):

$$\frac{d\sigma}{d\Omega} = \frac{r_0^2}{2} \left(\frac{\nu'}{\nu} \right)^2 A_0 \quad (2.8)$$

2.1. The ERF system

In this system the calculations of the coefficient F_0, the components of the vector $\boldsymbol{F}$ and the T-matrix elements, greatly simplify. With the positions

$$\nu = \frac{|\boldsymbol{k}|}{m}\,, \quad \nu' = \frac{|\boldsymbol{k}'|}{m}$$

and by indicating with θ the scattering angle, one has:

$$\tilde{s} = 2m^2 \nu\,, \quad \tilde{u} = -2m^2 \nu'\,, \quad \nu' = \frac{\nu}{1 + \nu(1 - \cos\theta)}\,.$$

Eqs. (2.5) become:

$$\xi_1^{(f)} = \frac{1}{A_0} \{ 2\,\xi_1^{(i)} \cos\theta + \xi_2^{(i)}\,\nu(1 - \cos\theta)\,(\boldsymbol{h} \cdot \boldsymbol{\zeta}) \}$$

$$\xi_2^{(f)} = \frac{1}{A_0}\Big\{ -\nu(1-\cos\theta)\,(\boldsymbol{f}'\cdot\boldsymbol{\zeta}) - \xi_1^{(i)}\,\nu'(1-\cos\theta)\,(\boldsymbol{h}\cdot\boldsymbol{\zeta}) + \xi_2^{(i)}\left(\frac{\nu}{\nu'}+\frac{\nu'}{\nu}\right)\cos\theta - \xi_3^{(i)}\,\nu'(1-\cos\theta)\,(\boldsymbol{g}\cdot\boldsymbol{\zeta})\Big\}$$

$$\xi_3^{(f)} = \frac{1}{A_0}\{ \sin^2\theta + \xi_2^{(i)}\,\nu(1-\cos\theta)\,(\boldsymbol{g}'\cdot\boldsymbol{\zeta}) + \xi_3^{(i)}\,(1+\cos^2\theta)\} \quad (2.9)$$

where

$$A_0 = \left(\frac{\nu}{\nu'}+\frac{\nu'}{\nu}-\sin^2\theta\right) + \xi_3^{(i)}\sin^2\theta - \xi_2^{(i)}\,\nu(1-\cos\theta)\,(\boldsymbol{f}\cdot\boldsymbol{\zeta}) \quad (2.10)$$

and

$$\boldsymbol{f} = \hat{k}\cos\theta + \hat{k}'\frac{\nu'}{\nu}, \quad \boldsymbol{f}' = \hat{k} + \hat{k}'\frac{\nu'}{\nu}\cos\theta$$
$$\boldsymbol{g} = \hat{k} - \hat{k}'\cos\theta, \quad \boldsymbol{g}' = \hat{k}\cos\theta - \hat{k}'$$
$$\boldsymbol{h} = \hat{k}\times\hat{k}' \quad (2.11)$$

In the case $\boldsymbol{\zeta} = 0$, Eqs. (2.9), (2.10) specialize in the known expressions:

$$\xi_1^{(f)} = \xi_1^{(i)}\,\frac{2\cos\theta}{A_0}$$
$$\xi_2^{(f)} = \xi_2^{(i)}\,\frac{\cos\theta}{A_0}\left(\frac{\nu}{\nu'}+\frac{\nu'}{\nu}\right)$$
$$\xi_3^{(f)} = \frac{1}{A_0}\{\sin^2\theta + \xi_3^{(i)}\,(1+\cos^2\theta)\} \quad (2.12)$$

where A_0 is given by

$$A_0 = \left(\frac{\nu}{\nu'}+\frac{\nu'}{\nu}-\sin^2\theta\right) + \xi_3^{(i)}\sin^2\theta \quad (2.13)$$

The same expressions are reported in Eqs. (3.13) of Ref. [4] and can be compared with Eqs. (2.12) and (2.13) by renaming the indices: $(1,2,3)_{\mathrm{AT}} \to (3,1,2)$). Since the components $\xi_1^{(f)}$ and $\xi_3^{(f)}$ are identical, we completely agree with Ref. [4] in the case of linearly polarized photons. On the contrary, the AT-value for $\xi_2^{(f)}$ is

$$\xi_2^{(f)}|_{\mathrm{AT}} = \frac{\cos\theta}{A_0}\left\{\left(\frac{\nu}{\nu'}+\frac{\nu'}{\nu}-2\right)\xi_1^{(i)} + 2\xi_2^{(i)}\right\} \quad (2.14)$$

which is incorrect, because it allows for a circular polarization component of the final photon even when the initial photon is purely linear ($\xi_2^{(i)} = 0$).

According to Eqs. (2.12), (2.13), the Stokes parameters do not show any explicit dependence upon the ϕ-emission angle of the final photon. As a matter of fact, this dependence is only hidden in the expressions of the unit vectors $\hat{\chi}_{1,2}^{(i)}$ and $\hat{\chi}_{1,2}^{(f)}$. In the reference system where the kinematics of the process is described:

$$\hat{k} = (0,\,0,\,1)$$
$$\hat{k}' = (\sin\theta\,\sin\phi,\,\sin\theta\,\cos\phi,\,\cos\theta)$$

Eqs. (2.2), (2.6) become

$$\hat{\chi}_1^{(i)} = (-\cos\phi,\,\sin\phi,\,0)\,, \quad \hat{\chi}_1^{(f)} = \hat{\chi}_1^{(i)}$$
$$\hat{\chi}_2^{(i)} = (-\sin\phi,\,-\cos\phi,\,0)$$
$$\hat{\chi}_2^{(f)} = (-\cos\theta\,\sin\phi,\,-\cos\theta\,\cos\phi,\,\sin\theta) \quad (2.15)$$

Since under a frame rotation, the Stokes parameters transform according to (ξ_2 is unaffected):

$$\xi_1' = \xi_1\cos2\beta + \xi_3\sin2\beta$$
$$\xi_3' = -\xi_1\sin2\beta + \xi_3\cos2\beta$$

a rotation of the two sets of unit vectors $\hat{\chi}^{(i,f)}$ of an angle $(\pi-\phi)$ transforms Eq. (2.12) into

$$s_1^{(f)} = \pm\frac{1}{A_0}\Big\{ -\sin^2\theta\sin2\phi + s_1^{(i)}\left[(1\mp\cos\theta)^2\sin^2 2\phi \pm 2\cos\theta\right] - \frac{1}{2}s_3^{(i)}\left[(1\mp\cos\theta)^2\sin4\phi\right]\Big\}$$
$$s_2^{(f)} = s_2^{(i)}\,\frac{\cos\theta}{A_0}\left(\frac{\nu}{\nu'}+\frac{\nu'}{\nu}\right)$$
$$s_3^{(f)} = \frac{1}{A_0}\Big\{\sin^2\theta\cos2\phi + \frac{1}{2}s_1^{(i)}\left[(1\mp\cos\theta)^2\sin4\phi\right] + s_3^{(i)}\left[(1\mp\cos\theta)^2\cos^2 2\phi \pm 2\cos\theta\right]\Big\} \quad (2.16)$$

with A_0 given by

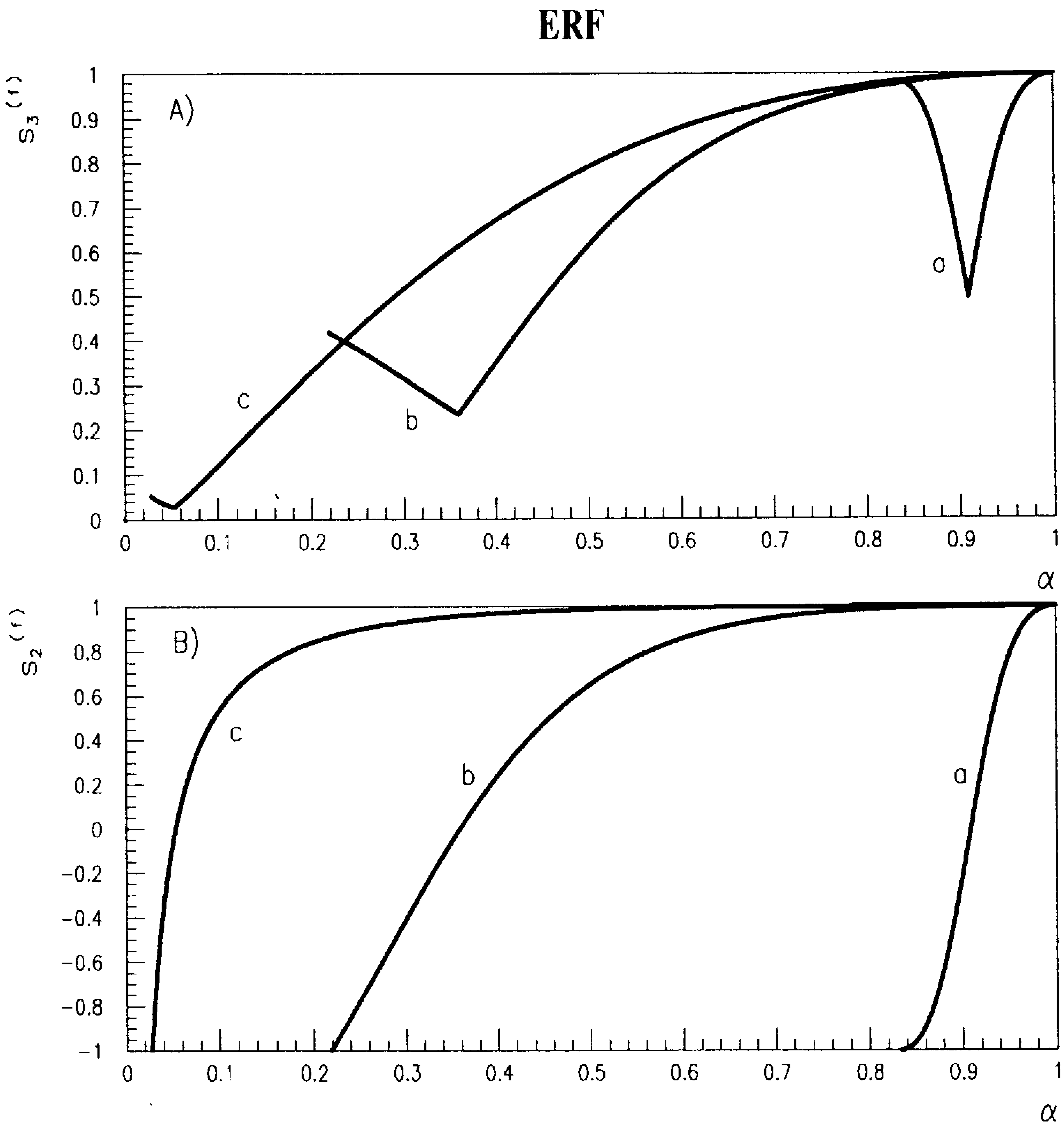

Fig. 1. ϕ-averaged Stokes parameters of the final photon as function of $\alpha = \nu'/\nu'_{max}$ in the ERF-system: A) $s_3^{(f)}$ for linearly polarized incident photon $s^{(i)} = (0,0,1)$; B) $s_2^{(f)}$ for circularly polarized incident photon $s^{(i)} = (0,1,0)$. The curves in each figure refer to three different values of the electron energy in the LAB-system: *a*) = 2.8 GeV; *b*) = 50 GeV; *c*) = 500 GeV.

$$A_0 = \left(\frac{\nu}{\nu'} + \frac{\nu'}{\nu} - \sin^2\theta\right) + (s_1^{(i)} \cos 2\phi + s_3^{(i)} \sin 2\phi)\sin^2\theta \qquad (2.17)$$

Here, the Stokes parameters $s^{(i)}$ and $s^{(f)}$ are still expressed in terms of two reference bases perpendicular to the corresponding photon momenta, but the unit vectors defined for the initial photon coincide with $\hat{x}$ and $\hat{y}$ of the reference system, whereas those of the final photon depend only upon θ. The double sign corresponds to the emission of the final photon in the forward (upper sign) and backward (lower sign) hemisphere, respectively. Since Eqs. (2.2), (2.6) assume that the third axis is oriented along the photon momentum and the unit vector $\hat{\chi}_2^{(f)}$ changes direction under reflection (see Eq. (2.15)), the final photon turns out to be described in systems with opposite handness when it is emitted forward or backward. This explains why the ϕ-dependence has to be taken with opposite signs when the photon is emitted in the two hemispheres. As for the circular polarization no ϕ-dependence is expected. Hence, no double sign appears in the expression for $s_2^{(f)}$ and a circularly polarized photon changes helicity passing from one hemisphere to the other.

On the experimental side, the final size of any practical detector requires an integration over its finite ϕ-acceptance. In particular for a round detector that monitors a backscattered laser beam, the ϕ-averaged val-

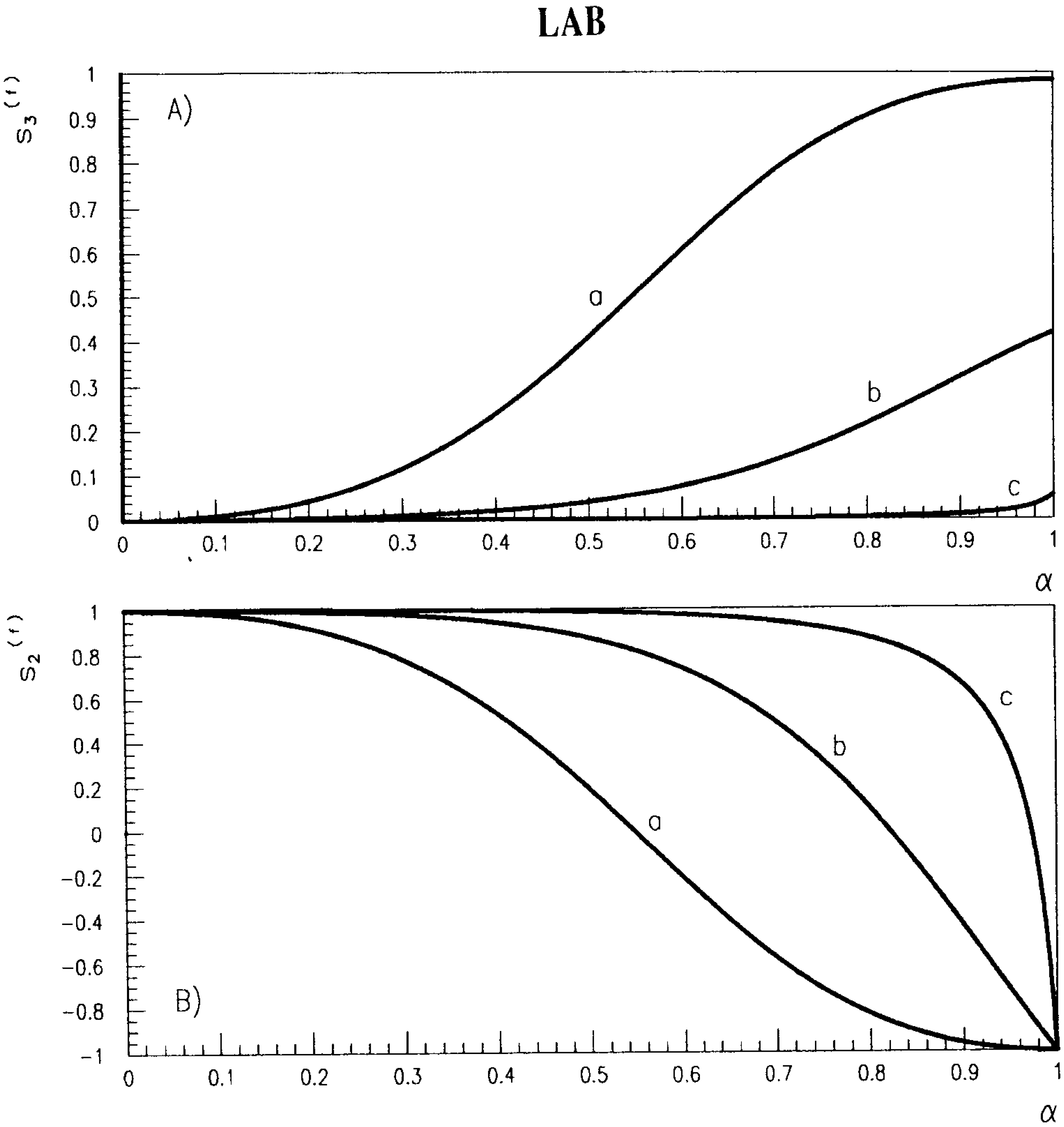

Fig. 2. The same as Fig. 1 in the LAB-system.

ues of the Stokes parameters are obtained by weighing Eqs. (2.16) with the differential cross section, and averaging over the full ϕ-range

$$< s^{(f)} > = \frac{\int_0^{2\pi} d\phi\, A_0 s^{(f)}}{\int_0^{2\pi} d\phi\, A_0} = \frac{\int_0^{2\pi} d\phi\, A_0 s^{(f)}}{< A_0 >}$$

yielding the results

$$< s_1^{(f)} > = \pm s_1^{(i)} \frac{(1 + |\cos\theta|)^2}{2 < A_0 >}$$
$$< s_2^{(f)} > = s_2^{(i)} \frac{\cos\theta}{< A_0 >} \left(\frac{\nu}{\nu'} + \frac{\nu'}{\nu} \right)$$
$$< s_3^{(f)} > = s_3^{(i)} \frac{(1 + |\cos\theta|)^2}{2 < A_0 >} \qquad (2.18)$$

where

$$< A_0 > = \frac{\nu}{\nu'} + \frac{\nu'}{\nu} - \sin^2\theta \qquad (2.19)$$

The curves a in Fig. 1 show the behaviour of the Stokes parameters of the final photon as function of the ratio $\alpha = \nu'/\nu'_{\rm max}$, when UV-photons from a frequency quadrupled Nd-YAG laser with λ = 266 nm (4.66 eV) collide against the electrons of the up-graded NSLS X-ray ring at BNL (E_e = 2.8 GeV) [6]. This behaviour can be understood from the analysis of the kinematical term appearing in Eqs. (2.18), (2.19). This factor can be rewritten in the following form:

$$\frac{\nu}{\nu'} + \frac{\nu'}{\nu} = 2 + \frac{\nu^2(1 - \cos\theta)^2}{1 + \nu(1 - \cos\theta)} \qquad (2.20)$$

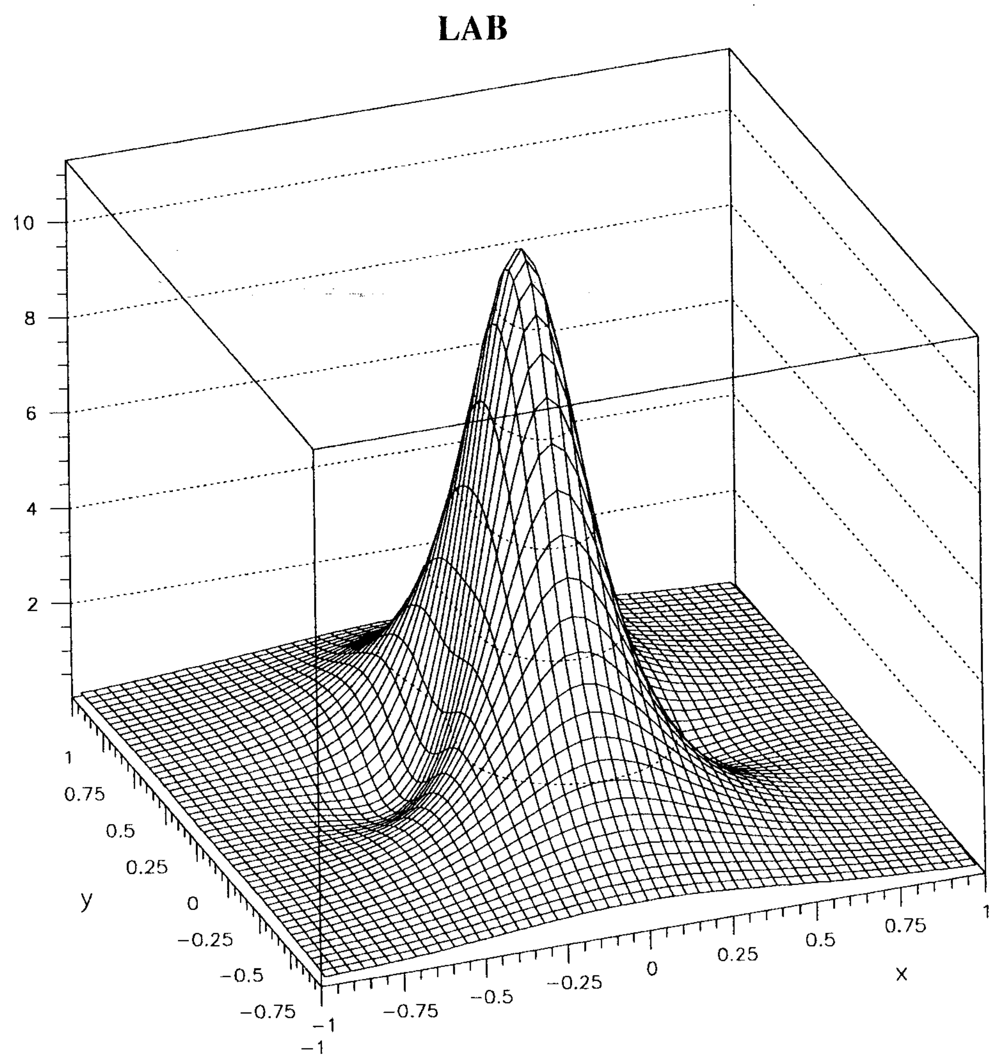

Fig. 3. Klein-Nishina differential cross-section $d^2\sigma/dxdy$, in units of r_0^2, in a plane transverse to the photon momentum in the LAB-system. The polarization vectors of the incoming particles are $[s^{(i)} = (0,0,1)]$ and $[\zeta = 0]$, respectively. The unit circle in the (x, y) plane corresponds to a cone of half-aperture $2/\gamma$.

and, for $\nu \ll 1$ it is always very close to 2, in the whole angular range. According to Eqs. (2.18), (2.19) the photons emitted inside the cone centered around $\theta = \pi$ ($\alpha = 0.833$, in case a of Fig. 1), retain almost the same degree of polarization of the initial photon. The cusp, present only in the case of linearly polarized photons, occurs at $\theta = \pi/2$ as a consequence of the absolute value appearing in Eqs. (2.18). In the case of incoming circularly polarized light (see Fig. 1B), the final photon maintains the helicity in forward hemisphere but scatters with opposite helicity in the backward hemisphere.

In the region $\nu \geq 1$, the kinematical factor of Eq. (2.20) increases with ν, giving rise to a corresponding decrease of the degree of linear polarization of the final photon. The curves b and c in Fig. 1A show that the drop of the linear polarization is dramatic when the electrons are in the multi-GeV region. This leads to the surprising conclusion that laser backscattering, at very high energy, cannot be considered as a good source of linearly polarized photons.

Thanks to the cancellation of the kinematical factor (2.20) in the second of Eqs. (2.18) at $\theta = 0, \pi$, this effect does not indeed occur for circularly polarized photons, as shown by curves b and c in Fig. 1B. This is clearly expected from angular momentum considerations, but disagrees quite strongly with the corresponding AT-result (third of Eqs. (3.25) of Ref. [4]):

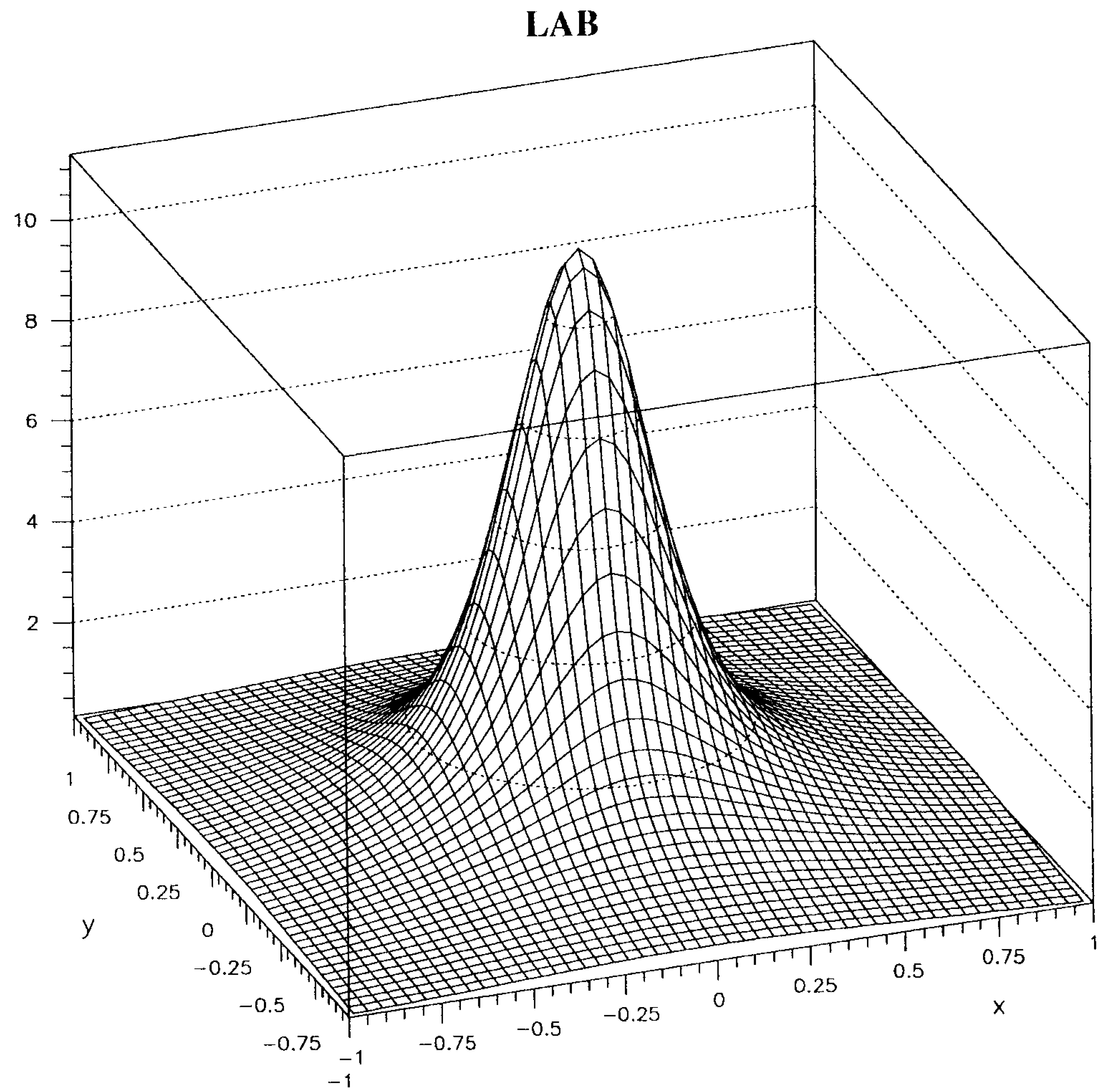

Fig. 4. The same as Fig. 3 for circularly polarized incoming photon [$s^{(i)} = (0,1,0)$].

$$< s_2^{(f)} > |_{AT} = s_2^{(i)} \frac{2\cos\theta}{< A_0 >} \qquad (2.21)$$

Here a fully circularly polarized photon is predicted to bounce back from the electron with a degree of circular polarization that, despite the angular momentum conservation, decreases with the increasing energy.

2.2. The LAB-system

On the experimental side it is definitely more convenient to look at the photon polarization in the LAB-system, where the real experiments are performed. However in this system the formalism discussed in Section 2.1 cannot be handled as easily as it has been done in the ERF-system.

Figs. 2 (curves a) show the behaviour of the linear and circular polarization of the LEGS photons, when the electron are unpolarized. Let us notice first that the value $\alpha = 1$ corresponds to backward scattering in the LAB but to forward scattering in the ERF-system. The Lorentz transformation that connects the two systems is such that the cusp profiles seen in Fig. 1A are so squeezed against the vertical axis that they are not visible in Fig. 2A. This result would be in strong disagreement with that of Ref. [4], if these authors really claim that the polarization profile is unaffected by the Lorentz transformation. And, indeed, this seems to be the case: the energy scale along the abscissa indicates that Fig. 22 of Ref. [4] refers to the LAB-system and the reported polarization degree exhibits the same cusp-like behaviour that we have found in the ERF-system. However, the definition of the linear polarization degree given in Ref. [4]

$$\bar{P}_l|_{AT} = \sqrt{< s_1 >^2 + < s_3 >^2} \qquad (2.22)$$

is not a Lorentz-invariant quantity. Therefore the results obtained in the LAB/ERF-systems must be different. In particular, for an incoming photon with $s^{(i)} = (0,0,1)$, Eq. (2.22) yield $\bar{P}_l|_{\rm AT} = < s_3^{(f)} >$ because $< s_1^{(f)} > = 0$ both in the ERF and LAB-systems. But, the Lorentz-invariant quantity defined in Eq. (2.1), yields for the LEGS case:

$$\bar{P}_l = \sqrt{< s_1^2 > + < s_3^2 >} \approx 1$$

in both systems, as expected. Therefore it is very likely that the incorrect LAB-behaviour quoted in Ref. [4] is due to an erroneous interpretation of Eq. (2.22). This evident discrepancy does not show up in the backward direction where the LEGS-type experiments usually operate. It would appear as a huge effect around $\theta^{(\rm ERF)} \approx \pi/2$. At present, no data are available to check this conclusion.

Fig. 3 shows the transverse spatial distribution of the backscattered photons in the present LEGS conditions: linearly polarized light against unpolarized electrons. According to the structure of the Klein-Nishina formula, the two dips, clearly visible in Fig. 3, line up with the polarization direction of the initial photons and disappear completely in Fig. 4 where the same distribution is shown for circular photons.

Finally, with the help of Eqs. (2.9), (2.10) we can extend these considerations to the case where the electrons are polarized either longitudinally or transversly to the direction of the incoming photon: any other polarization state can be reconduced to a combination of these two basic states.

Electrons in a storage ring can build up a partial transverse polarization as a result of the combined action of the polarizing synchrotron radiation and the depolarizing effect due to the magnetic lattice imperfections. The ζ-dependent term in Eqs. (2.10) shows that the electron transverse polarization can be measured with circularly polarized photons, by looking at the ϕ-asymmetry in the distribution of the scattered photons. This opportunity has been repeatedly used to measure the electron transverse polarization in several storage rings (SPEAR, LEP, HERA) [9]. However, the ϕ-averaged polarization of the final photon is completely insensitive to the electron transverse polarization.

The greatest interest arises when the electrons are longitudinally polarized. In Ref. [10] we showed that unpolarized photons acquire some small degree of circular polarization ($\approx$ 20 % in the ERF) when they are scattered off longitudinally polarized electrons. Moreover, when the laser photons are circular, the two electron helicity states determine different values for the circular polarization of the final photons, as reported also in Ref. [5]. This difference amplifies considerably at high energy [10].

References

[1] L.D. Landau and E.M. Lifšits, Relativistic Quantum Theory, Part 1 (Pergamon Press, 1971) p. 301.

[2] U. Fano, J. Opt. Soc. Am. 39 (1949) 859.

[3] F.W. Lipps and H.A. Tolhoek, Physica XX (1954) 395.

[4] F.R. Arutyunian and V.A. Tumanian, Sov. Phys. Usp. 83 (1964) 339; Phys. Lett. 4 (1963) 177.

[5] Y.S. Tsai, Phys. Rev. D 48 (1993) 96.

[6] C.E. Thorn et al., Nucl. Instr. Meth., A 285 (1989) 447.

[7] D. Babusci et al., Nuovo Cimento 103 (1990) 1555.

[8] LEGS-Spin Collaboration (D. Babusci et al.), BNL-61005 (1994).

[9] D.B. Gustavson et al., Nucl. Instr. Meth. 165 (1979) 177; L. Knudsen et al., Phys. Lett. B 270 (1991) 97, and references quoted therein.

[10] D. Babusci, G. Giordano and G. Matone, LNF–95/004 (IR) (1995).